NASA TECHNICAL NOTE

NASA TN D-6071

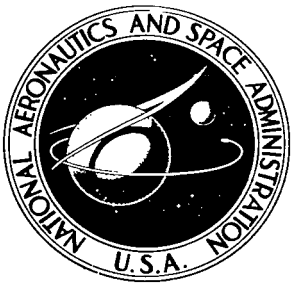




# EFFECT OF SIMULATED DOWNSTREAM FLOW BLOCKAGE DOORS ON THE PERFORMANCE OF AN AXIAL-FLOW FAN ROTOR

*by Walter M. Osborn and Jack M. Wagner*

*Lewis Research Center*
*Cleveland, Ohio 44135*

NATIONAL AERONAUTICS AND SPACE ADMINISTRATION • WASHINGTON, D. C. • NOVEMBER 1970

| | |
|---|---|
| 1. Report No. NASA TN D-6071 | 2. Government Accession No. |
| 4. Title and Subtitle EFFECT OF SIMULATED DOWNSTREAM FLOW BLOCKAGE DOORS ON THE PERFORMANCE OF AN AXIAL-FLOW FAN ROTOR | 5. Report Date November 1970<br>6. Performing Organization Code |
| 7. Author(s) Walter M. Osborn and Jack M. Wagner | 8. Performing Organization Report No. E-5215 |
| 9. Performing Organization Name and Address Lewis Research Center, National Aeronautics and Space Administration, Cleveland, Ohio 44135 | 10. Work Unit No. 720-13<br>11. Contract or Grant No. |
| 12. Sponsoring Agency Name and Address National Aeronautics and Space Administration, Washington, D.C. 20546 | 13. Type of Report and Period Covered Technical Note<br>14. Sponsoring Agency Code |
| 15. Supplementary Notes | |

16. Abstract

Two downstream flow blockages simulating door positions of $20^{\circ}$ and $45^{\circ}$ in the bypass air duct of a turbofan engine were tested with an axial-flow fan rotor. The rotor performance was stable and repeatable, and both configurations suppressed rotating stall. At the minimum flow points, an increase in inlet temperature in the tip region indicated the existence of an eddy flow. Temperatures remained within operational limits. Reductions in torque and flow rate with the $45^{\circ}$ blockage ring indicated that a flow blockage device might ease engine starting requirements and might be used to reduce engine thrust while maintaining high engine speed.

| | | | |
|---|---|---|---|
| 17. Key Words (Suggested by Author(s)) Compressors, Flow blockage, Turbofan engines | 18. Distribution Statement Unclassified - unlimited | | |
| 19. Security Classif. (of this report) Unclassified | 20. Security Classif. (of this page) Unclassified | 21. No. of Pages 26 | 22. Price* $3.00 |

*For sale by the Clearinghouse for Federal Scientific and Technical Information
Springfield, Virginia 22151

# EFFECT OF SIMULATED DOWNSTREAM FLOW BLOCKAGE DOORS ON THE PERFORMANCE OF AN AXIAL-FLOW FAN ROTOR

by Walter M. Osborn and Jack M. Wagner

Lewis Research Center

## SUMMARY

An investigation was made to determine the effects of downstream flow blockage on the performance of an axial-flow fan rotor. Two fixed blockage rings that simulated movable door positions of $20^{\circ}$ and $45^{\circ}$ in the bypass air duct of a turbofan engine were tested. Rotor performance was stable and repeatable. Both configurations suppressed rotating stall at equivalent speeds as high as 0.7 $N_D$ (977 ft/sec or 298 m/sec tip speed), which indicated that movable doors might be used as a practical device for blocking the fan stage bypass air. The maximum vibratory blade stress was ±5500 psi ($37.92 \times 10^6$ $N/m^2$).

Rotor inlet temperature profiles for the minimum flow points for both configurations showed much higher temperatures at the blade tip than at the blade hub. This indicates the presence of an eddy condition or backflow near the blade tip. The temperature remained within operational limits ($703^{\circ}$ R or 390.5 K max). At low flows, the eddy was larger for the $45^{\circ}$ configuration and mixed more with the main stream. As the flow was increased to the maximum efficiency point, the eddy disappeared at the upstream measuring station for the $20^{\circ}$ configuration but persisted for the $45^{\circ}$ configuration.

The torque reductions obtained with the simulated $45^{\circ}$ and $90^{\circ}$ (ref. 1) door positions suggest starting the engine with the fan bypass air blocked to reduce the starting torque requirements. Such torque reductions might permit the use of smaller and, therefore, lower cost components in the starting systems.

At 0.7 $N_D$ and a simulated door position of $45^{\circ}$, the core gas generator would be subjected to a change in pressure ratio from 1.306 (unblocked) to 1.247 and a loss in maximum efficiency of approximately 30 percentage points. The losses are slightly higher for the simulated $90^{\circ}$ door position (ref. 1).

The substantial flow reductions obtained for the $45^{\circ}$ and $90^{\circ}$ door positions suggest using a flow blockage device as a means of controlling thrust while maintaining high engine speed.

# INTRODUCTION

Turbofan engines may benefit from a reduction in flow and fan power during starting and low-thrust operation. Because the inlet air flow of a turbofan engine is separated into fan air and gas generator (core engine) air, this engine is particularly adaptable to blocking the fan air flow to obtain such reductions. By suppressing rotating stall in the fan stage rotor, a flow blockage device may be used to improve the operational stability at off-design speeds (ref. 2). Thus, improvement in overall engine operation and possibly engine acceleration characteristics might be obtained (ref. 3). A reduction in rotor torque due to flow blockage could ease engine starting requirements and enable low cost components to be used in the engine starting system. Also, flow reductions obtained with blockage might enable a flow blockage device to be used for controlling thrust for maneuvers where low thrust and high engine rpm are desirable.

To obtain the aforementioned benefits, a method (ref. 1) was investigated that made use of tip annulus flow blockage downstream of a fan-type axial-flow rotor. Such blockage could be used as a device to block the fan bypass air. Three flow blockages, 22, 55, and 75 percent (inserted perpendicularly to the flow streamlines close behind the rotor), were used in the tests and could be considered as a simulation of a range of core engine sizes or as bypass air ratios. In the tests, each of the blockage rings suppressed rotating stall at speeds as high as 0.7 of design and enabled the rotor to operate in a stable condition at much lower flows than were possible with the unblocked passage. Thus, improved acceleration potential and engine operation might result. Substantial reductions in rotor torque and flow rate were obtained.

A fan engine flow blockage device might take the form of a series of hinged overlapping doors or flaps that could be actuated to block the bypass air. The blockage configurations used in reference 1 would represent the doors in the fully extended or $90^{\circ}$ position. However, the doors must be actuated through an arc from $0^{\circ}$ to $90^{\circ}$, and the rotor performance must be stable through the transition positions for such a device to be successfully used.

The purpose of this investigation was to determine the effect of downstream flow blockage at simulated door positions of $20^{\circ}$ and $45^{\circ}$ on the performance of the axial-flow rotor used in the investigation of reference 1. Particular emphasis was placed on observing the efficiency, torque reduction, flow reduction, pressure-ratio maintenance, and stability of operation. The rotor with blockage rings was tested over a speed range of 0.3 to 0.7 of design speed and the flow range obtainable by changing the facility outlet flow control valve setting from the fully open to the fully closed position.

## SYMBOLS

| | |
|---|---|
| N | actual rotor speed, rpm |
| $N_D$ | equivalent design speed, $N/\sqrt{\theta}$, 16 000 rpm |
| T | total temperature (corrected to standard day conditions) |
| W | actual air weight flow, lbm/sec (kg/sec) |
| $\delta$ | ratio of inlet (plenum) total pressure to NACA standard sea-level pressure of 29.92 inches of Hg abs ($1.01\times10^5$ N/m$^2$ abs) |
| $\eta_{ad}$ | adiabatic temperature-rise efficiency |
| $\theta$ | ratio of inlet (plenum) total temperature to NACA standard sea-level temperature of 518.7$^\circ$ R (288.2 K) |

## APPARATUS AND PROCEDURE

A schematic diagram of the test facility is shown in figure 1. The drive system, instrumentation, and test rotor were the same as those used for the tests of reference 1.

A photograph of the test rotor is shown in figure 2. The rotor had 47 blades, a nominal diameter of 20 inches (50.8 cm), and a hub-tip radius ratio of 0.5 at the inlet. The design tip diffusion factor was 0.45, and the equivalent design operating speed $N_D$ was 16 000 rpm or an inlet tip speed of approximately 1396 feet per second (426 m/sec). The rotor was equipped with blade vibration dampers (fig. 2), and 10 blades were instrumented with strain gages to monitor the blade stress during the investigation.

Profiles of the two blockage rings used in the tests are shown in figure 3. The aluminum rings were cut at angles of 20$^\circ$ and 45$^\circ$. The corresponding flow blockages were 25.2 and 47.8 percent, respectively. A flow divider ring was placed immediately downstream of the rotor and in line with the blade vibration dampers (fig. 3). This placement simulates a division of the air flow into bypass air outside the dampers and core engine air inside the dampers. The divider ring was fastened to the outer shrouding by four spacers. The length of the angle cut (door length) was chosen so that in a 90$^\circ$ door position the total air flow above the blade vibration dampers (bypass air) would be blocked. The data presented in reference 1 for the 55-percent flow blockage are representative of the rotor performance with the door in the 90$^\circ$ position or completely blocked bypass air.

All tests were conducted using atmospheric air at the rotor inlet. The inlet flow control valve was in the fully open position throughout the tests. Vacuum exhaust was used at the rotor outlet to help overcome the system losses. The partially blocked

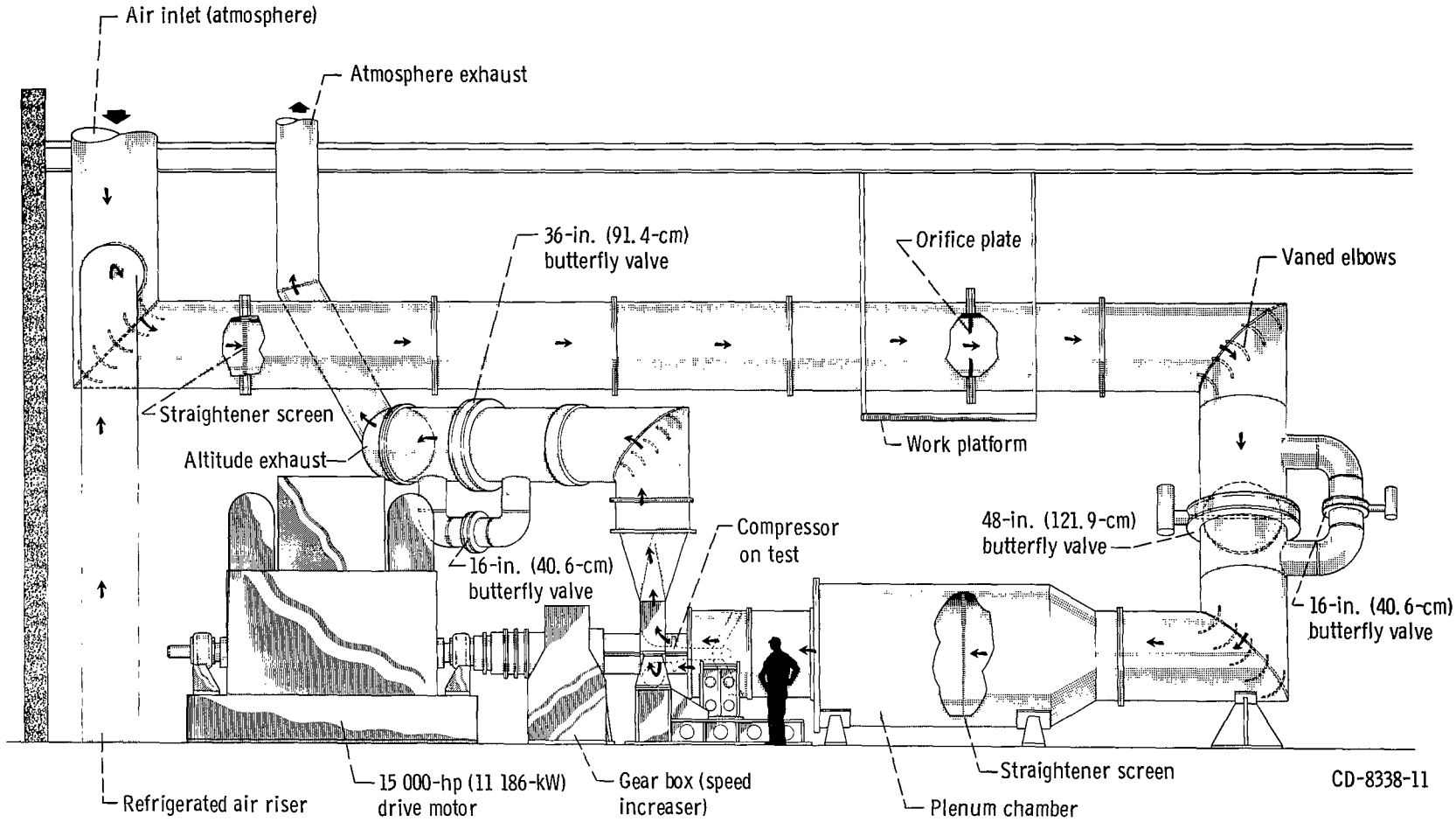


Figure 1. - Test facility.

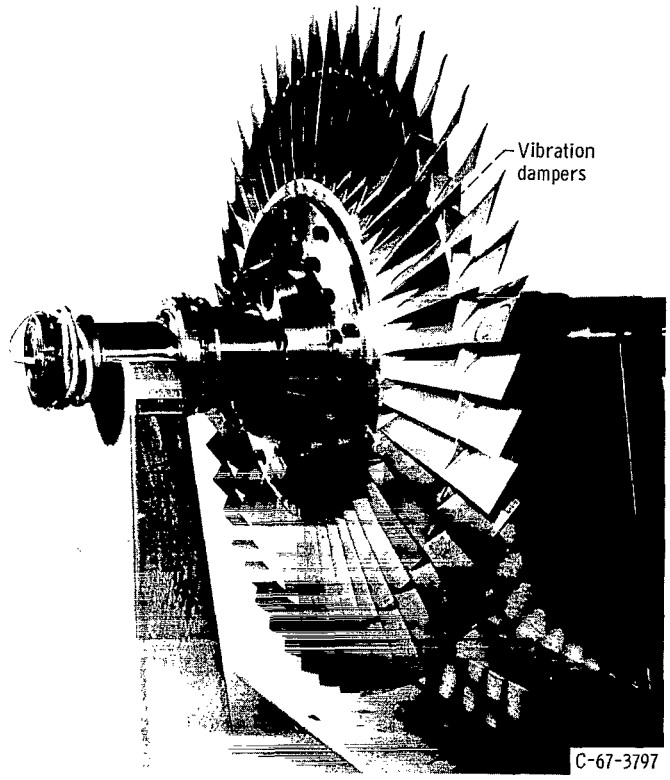


Figure 2. - 20-Inch (50.8-cm) axial-flow fan rotor.

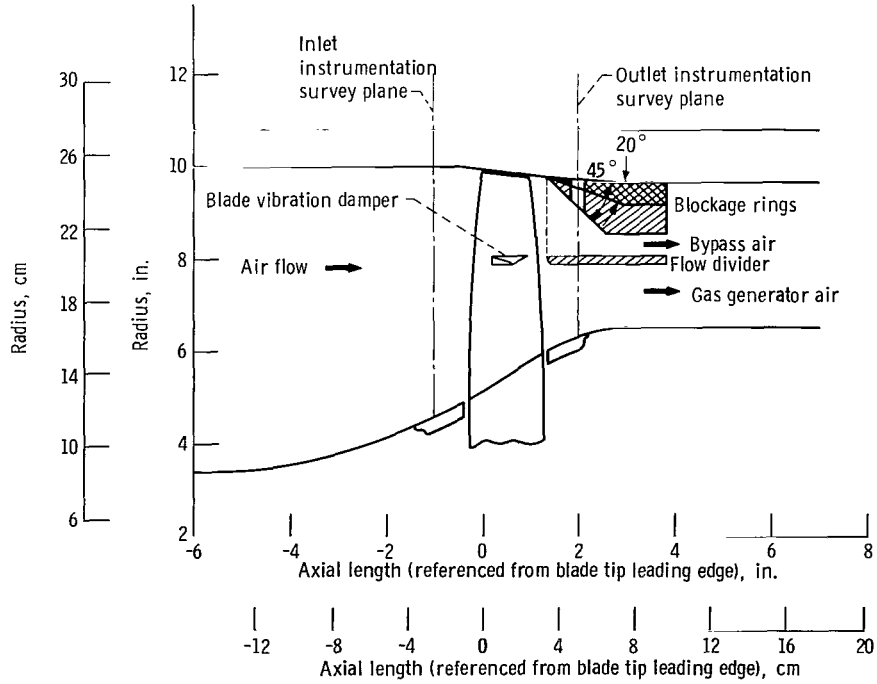


Figure 3. - Meridional view of axial-flow rotor and 20° and 45° blockage rings.

rotor was tested over a range of speeds from 0.3 to 0.7 $N_D$. The blockage tests were limited to a maximum rotor speed of 0.7 $N_D$, or a tip speed of approximately 977 feet per second (298 m/sec), because this tip speed is probably representative of many commercial engines. The flow range was obtained by changing the outlet flow control valve setting from the fully open to the fully closed position.

The overall rotor performance is based on average conditions in the inlet plenum tank and mass-averaged values of outlet temperature and pressure. The rotor outlet conditions were determined by radial surveys taken approximately 1 inch (2.54 cm) downstream from the blade tip trailing edge (fig. 3). Inlet radial surveys of temperature were also taken 1 inch (2.54 cm) upstream of the blade tip leading edge (fig. 3). All performance parameters were based on measurements corrected to standard day conditions. The rotor torque was calculated from the equivalent weight flow, rotor rpm, and the total temperature ratio (ratio of absolute values of outlet total temperature to plenum total temperature).

A radially traversing hot-wire anemometer probe located 1 inch (2.54 cm) upstream of the blade tip leading edge (fig. 3) was used to determine the existence of rotating stall.

## RESULTS AND DISCUSSION

The results of this investigation are presented in four main sections: (1) rotor performance without flow blockage, (2) rotor performance with blockage simulating a $20^{\circ}$ door position, (3) rotor performance with blockage simulating a $45^{\circ}$ door position, and (4) rotor performance comparison of unblocked and blocked configurations.

### Rotor Performance Without Annulus Area Blockage

The rotor performance without blockage was obtained from reference 1 and is repeated herein for convenience in making a comparison with the blocked rotor performance. The unblocked rotor was tested without the flow divider ring (fig. 3). The rotor performance is shown in figure 4 as curves of pressure ratio, efficiency, and torque as a function of equivalent weight flow for various fractions of design speed ($N_D$ = 16 000 rpm) from 0.4 to 1.0. At design speed, a maximum efficiency of 0.846 was obtained at a pressure ratio of 1.80 and an equivalent weight flow of 63.50 pounds per second (28.8 kg/sec).

Rotor performance to the left of the stall line (at lower weight flows) was explored at 0.4 to 0.7 $N_D$. Hot-wire anemometer surveys at the rotor inlet indicated the existence of rotating stall over the short dashed portions of the performance curves. At the

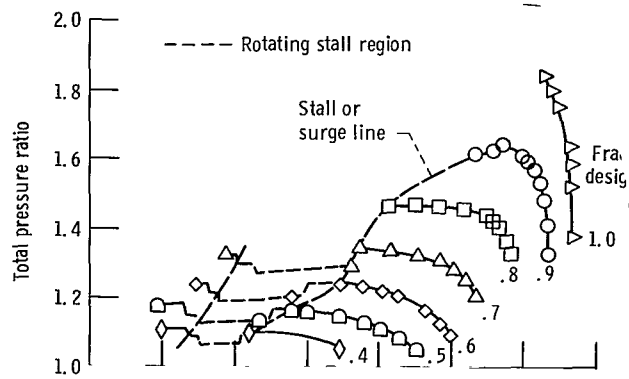


(a) Total pressure ratio as function of weight flow.

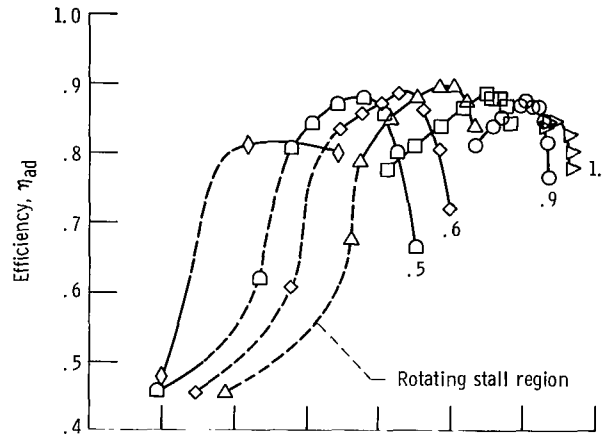


(b) Efficiency as function of weight flow.

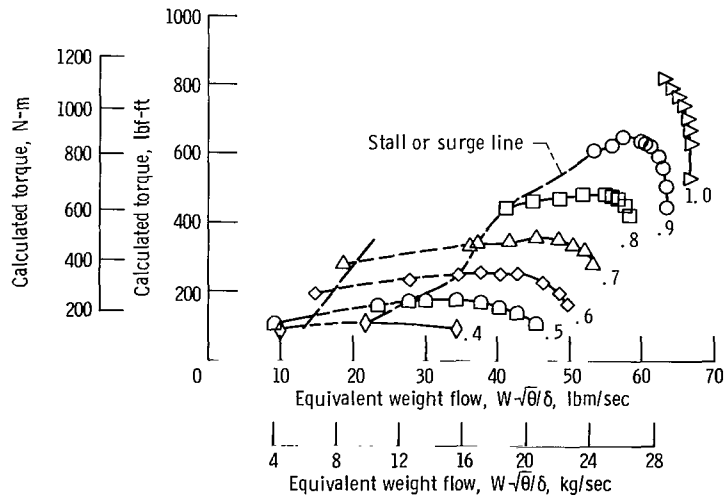


(c) Torque as function of weight flow.

Figure 4. - Rotor performance without blockage.

lowest weight flow points (end points) for all the performance curves at rotating speeds from 0.4 to 0.7 $N_D$, rotating stall disappeared, and rotor operation was stable. There was a slight recovery in pressure ratio of those points, but the efficiency was low (≈0.46).

## Rotor Performance for Simulated 20° Door Position

The performance curves for rotor with a 20° blockage ring are shown in figure 5. Pressure ratio, efficiency, torque, and temperature ratio are presented as functions of equivalent weight flow for speeds from 0.3 to 0.7 $N_D$.

In general, the performance parameters are slightly degraded from those of the unblocked rotor, except for the ability of the blocked rotor to operate in a stable condition to much lower flows. No evidence of rotating stall was detected by hot-wire anemometer surveys at the inlet to the rotor even at the minimum flow points at speeds as high as 0.7 $N_D$ (≈977-ft/sec or 298-m/sec tip speed). Also, the minimum points of figure 5 do not represent a stall limit or the minimum flow operating point for the blocked rotor. The mimum flow at each speed is the flow that leaked by the closed outlet flow control valve with the facility altitude exhaust system in use.

The maximum adiabatic efficiencies (fig. 5(b)) were between 0.824 and 0.853 for the speeds investigated. The maximum efficiency at each speed is relatively high, which indicates that the 20° blockage ring did not significantly distort the flow pattern at these points. The efficiencies for the maximum flow points for 0.3 and 0.4 $N_D$ are not shown because they were less than 0.40. The efficiency curves for these speeds are shown as short dashed lines between the maximum flow and the next lower weight flow data point because the efficiencies are not well defined. Low efficiencies are indicated at the minimum flow points even though hot-wire anemometer surveys at the rotor inlet indicated no rotating stall patterns.

The rotor inlet radial temperature distributions for 0.5 and 0.7 $N_D$ are shown in figure 6 for both the minimum flow points (maximum temperature variation) and the maximum efficiency points. At the minimum flow points for both speeds (figs. 6(a) and (b)), the inlet temperature is approximately the same as the upstream plenum temperature (518.7° R or 288,2 K) near the blade hub, but it increases toward the blade tip. The rate of increase of temperature with radius was greater at 0.7 $N_D$ than at 0.5 $N_D$, and a maximum temperature of approximately 700° R (388.7 K) was reached near the blade tip at 0.7 $N_D$. These inlet temperature profiles are probably indicative of a recirculation flow (eddy) near the blade tip caused by the inserted downstream flow blockage. Although hot-wire anemometer surveys at the rotor inlet gave no indication of rotating stall, it is possible that the high streamline curvatures in the tip region (due to

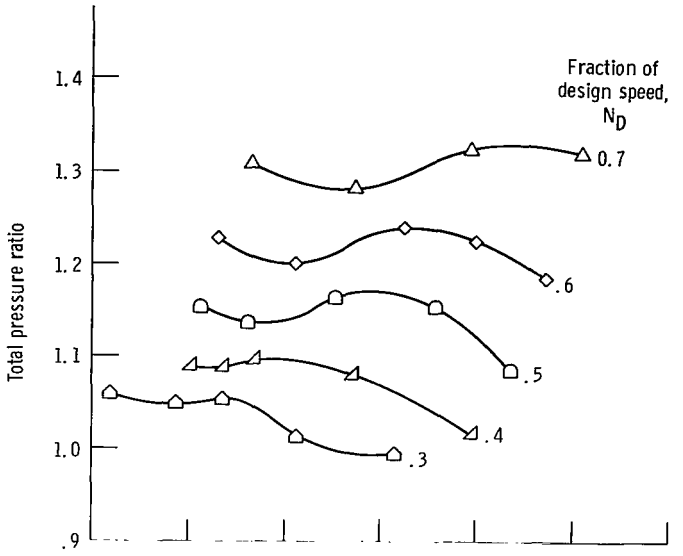


(a) Total pressure ratio as function of weight flow.

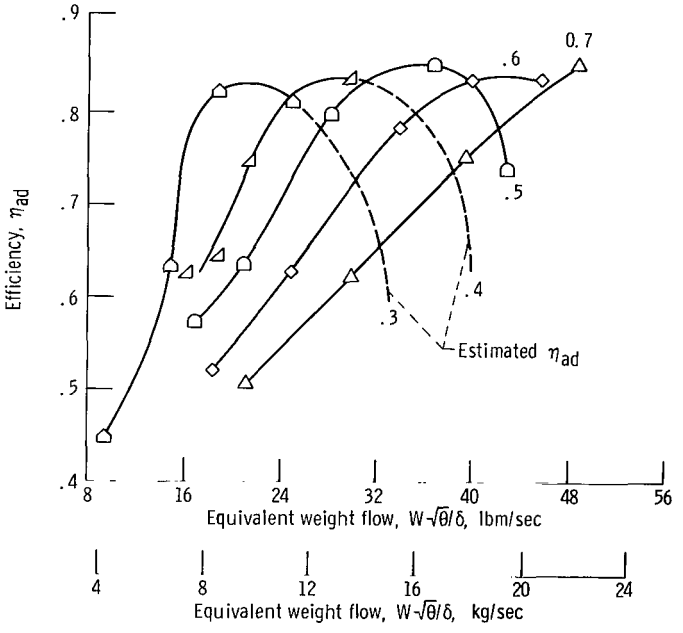


(b) Efficiency as function of weight flow.

Figure 5. - Rotor performance with 20° flow blockage ring.

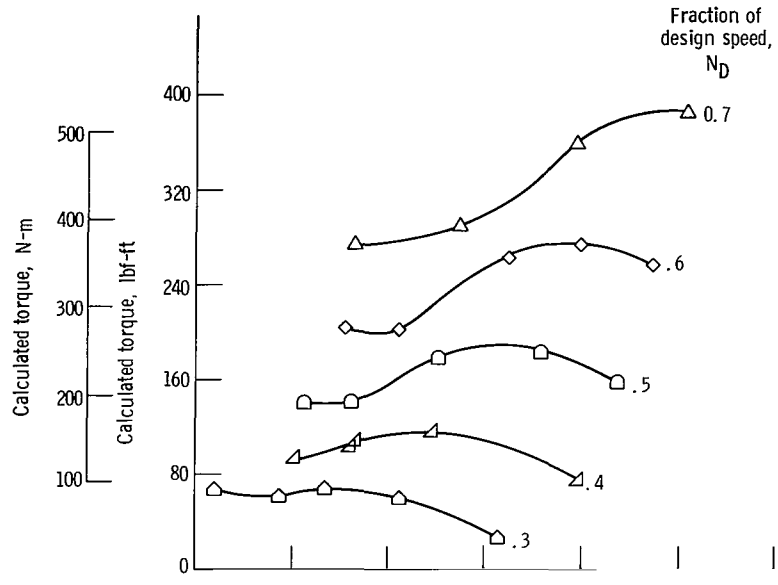


(c) Torque as function of weight flow.

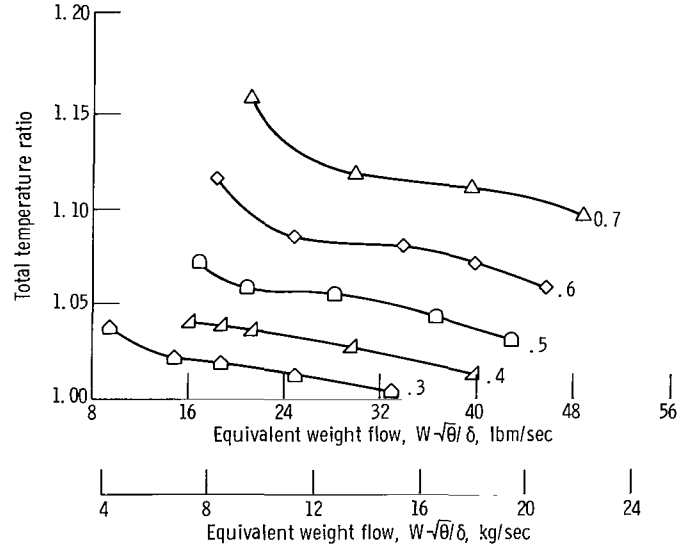


(d) Total temperature ratio as function of weight flow.

Figure 5. - Concluded.

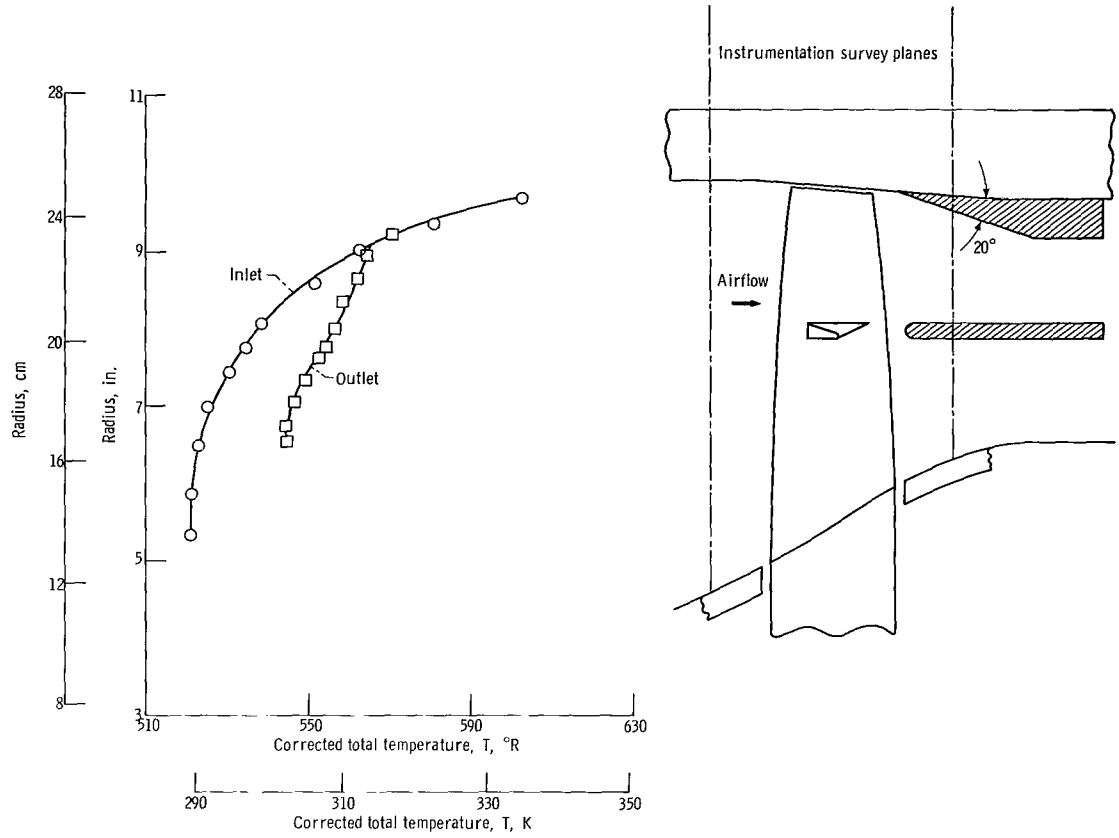


(a) Equivalent speed, 0.5 $N_D$; minimum flow point, 16.9 pounds mass per second (7.7 kg/sec).

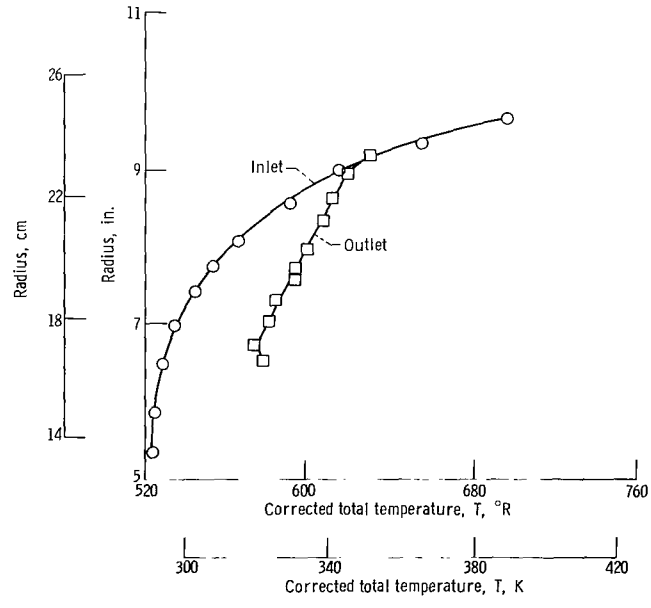


(b) Equivalent speed, 0.7 $N_D$; minimum flow point, 21.1 pounds mass per second (9.6 kg/sec).

Figure 6. - Inlet and outlet total temperature profiles for rotor with blockage simulating 20° door position.

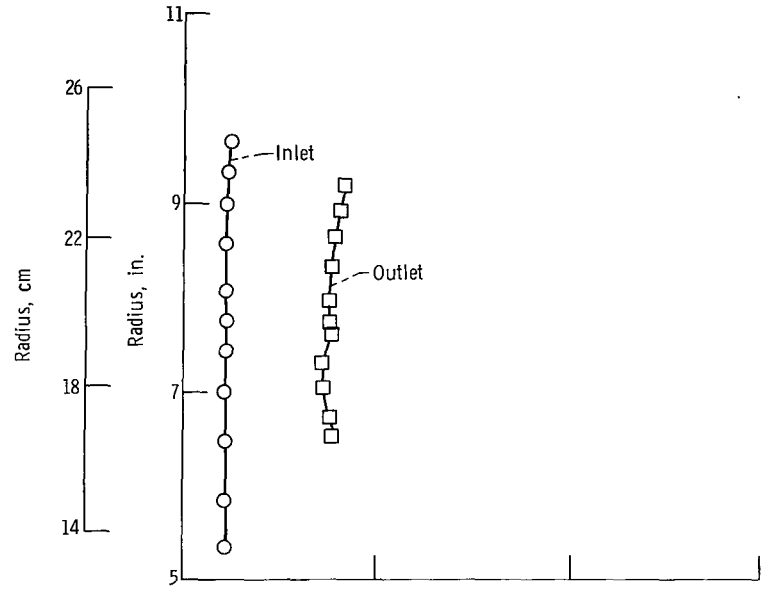


(c) Equivalent speed, 0.5 $N_D$; maximum efficiency point; 36.5 pounds mass per second (16.6 kg/sec).

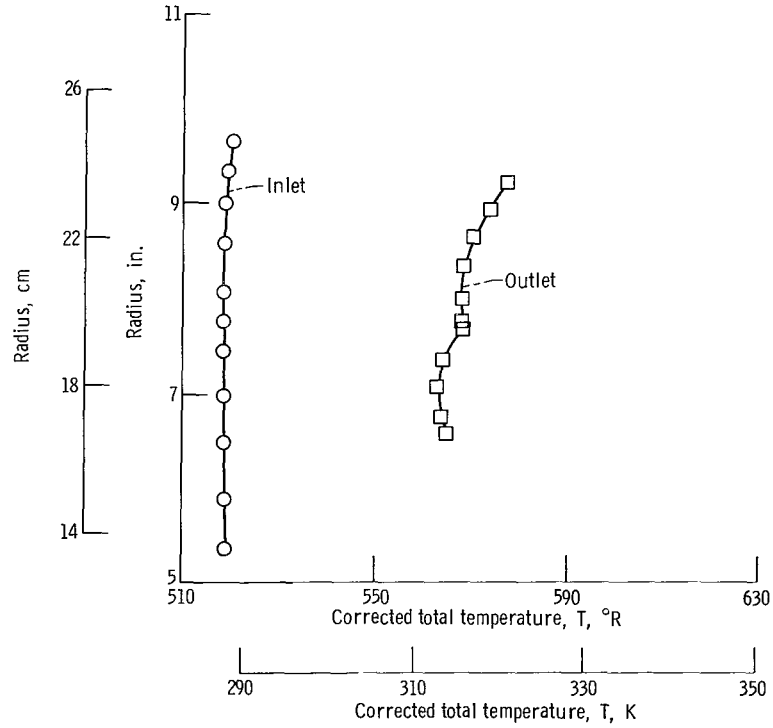


(d) Equivalent speed, 0.7 $N_D$; maximum efficiency point, 48.6 pounds mass per second (22.0 kg/sec).

Figure 6. - Concluded.

the eddy) resulted in another type of stall, such as ring stall. Such stalled operation could account for the low efficiencies evidenced at the minimum flow points.

The outlet temperature profiles for the minimum flow points (figs. 6(a) and (b)) also show an increase in temperature with increasing radius, but the temperature gradients are not as large as those at the inlet.

For the maximum efficiency points at 0.5 and 0.7 $N_D$ (figs. 6(c) and (d)), there was essentially no variation in inlet temperature, and the temperature was approximately the same as the plenum temperature (518.7° R or 288.2 K). Thus, little or no eddy flow exists at the inlet measuring station. The maximum efficiency is approximately 5 percentage points lower than the unblocked maximum efficiency. At 0.5 $N_D$, the outlet temperature was nearly constant with increasing radius, while an increase of approximately 14° R (7.8 K) was observed at 0.7 $N_D$.

## Rotor Performance for Simulated 45° Door Position

The performance curves for the rotor with a 45° blockage ring are shown in figure 7. Again, the minimum flow points are the result of a facility limitation and do not represent a stall limit or the minimum flow operating point for the blocked rotor. No evidence of rotating stall was detected.

The maximum adiabatic efficiencies (fig. 7(b)) are between 0.599 and 0.66 for the speeds investigated, with the highest efficiency occurring at 0.4 $N_D$. These efficiencies are much lower than those obtained with the 20° blockage ring, which indicates a greater level of flow distortion.

A discontinuity is shown in the torque curves (fig. 6(c)) wherein the torque increases quite rapidly for a small decrease in weight flow. Similar discontinuities were observed in the investigation of reference 1 and were believed to be associated with a change in the eddy flow characteristics.

The rotor inlet and outlet radial temperature distributions for 0.5 and 0.7 $N_D$ are shown in figure 8 for both the minimum flow points (maximum temperature variation) and the maximum efficiency points. At the minimum flow points (figs. 8(a) and (b)), the temperature profiles are similar to those for the 20° blockage ring. The inlet temperature increases from the hub to the tip. A maximum temperature of approximately 703° R (390.5 K) was reached near the blade tip at 0.7 $N_D$ because of the eddy flow in this region. For the 45° blockage ring, the temperature near the blade hub is higher than the upstream plenum temperature, which indicates a larger eddy flow and more mixing between the eddy flow and main stream flow than was obtained for the 20° blockage ring. The outlet temperature profiles for the minimum flow points (figs. 8(a) and (b)) also show an increase in temperature from the hub to the tip.

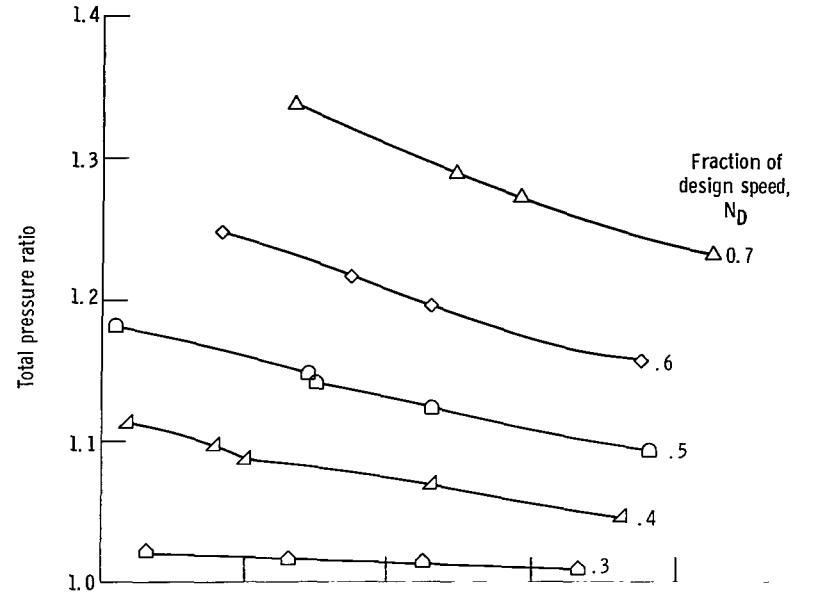


(a) Total pressure ratio as function of weight flow.

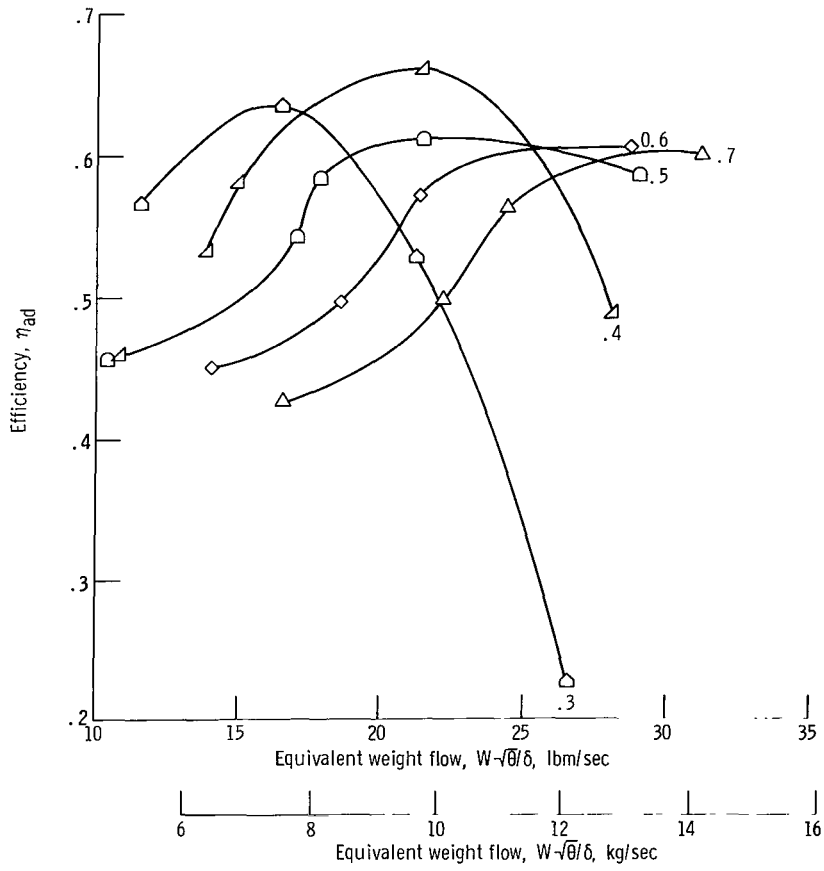


(b) Efficiency as function of weight flow.

Figure 7. - Rotor performance with flow blockage simulating 45° door position.

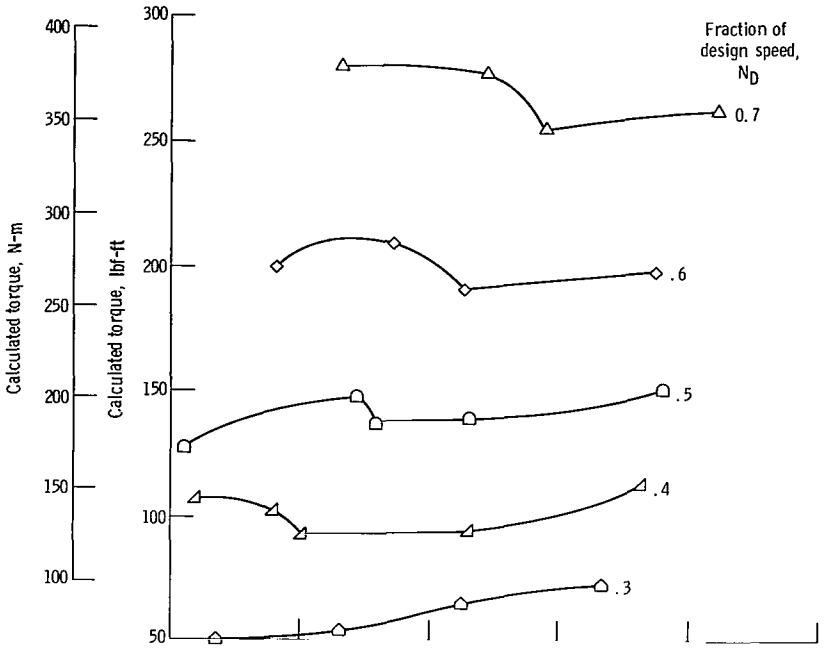


(c) Torque as function of weight flow.

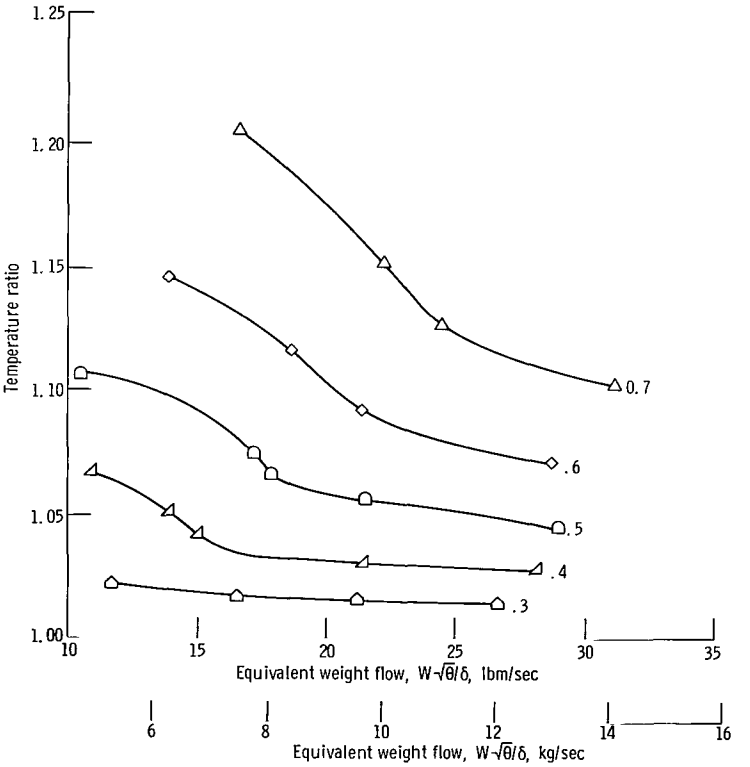


(d) Total temperature ratio as function of weight flow.

Figure 7. - Concluded.

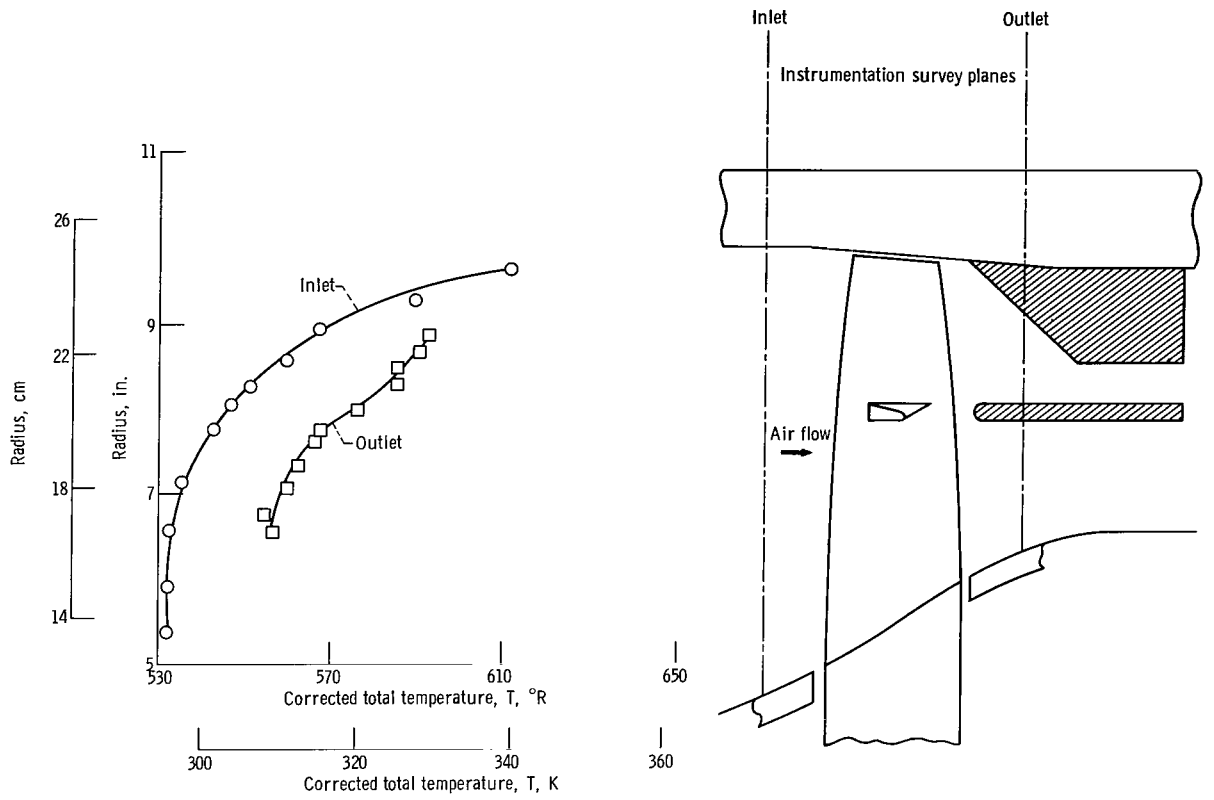


(a) Equivalent design speed, 0.5; minimum flow point (equivalent weight flow), 10.5 pounds mass per second (4.75 kg/sec).

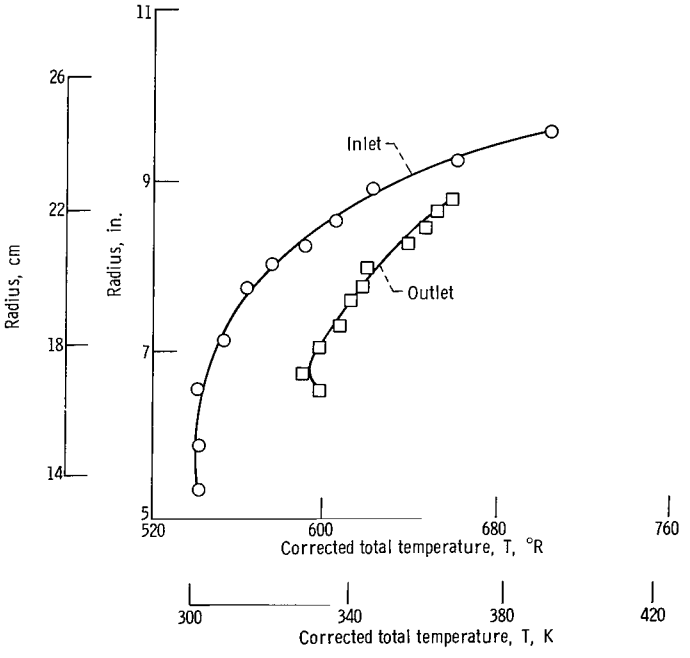


(b) Equivalent design speed, 0.7; minimum flow point (equivalent weight flow), 16.55 pounds mass per second (7.5 kg/sec).

Figure 8. - Inlet and outlet total temperature profiles for rotor with blockage simulating 45° door position.

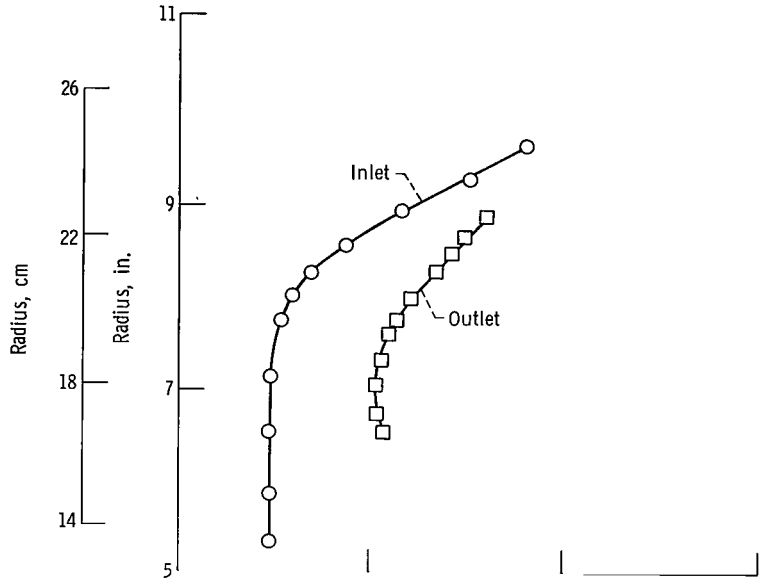


(c) Equivalent speed, 0.5 $N_D$; maximum efficiency point (equivalent weight flow), 21.5 pounds mass per second (9.75 kg/sec).

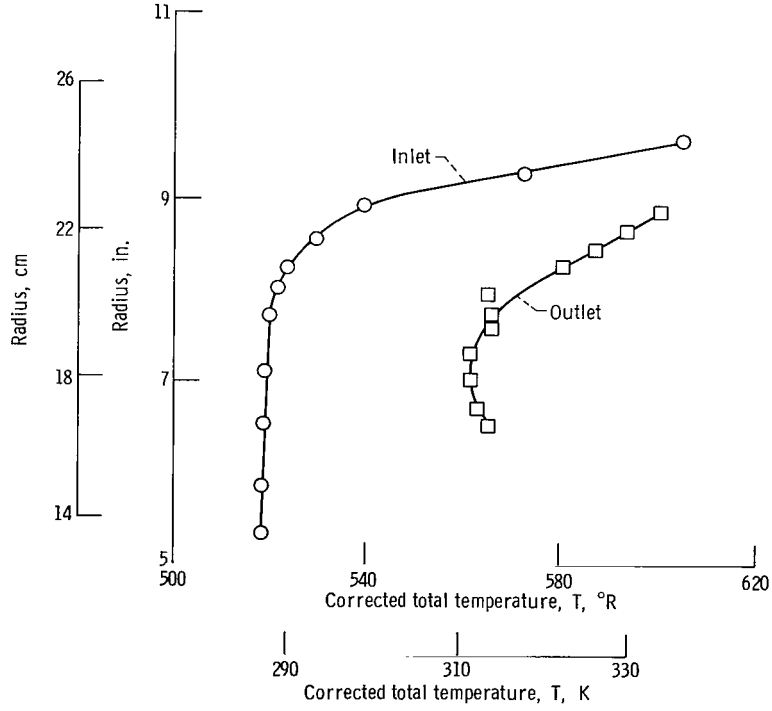


(d) Equivalent speed, 0.7 $N_D$; maximum efficiency point (equivalent weight flow), 31.1 pounds mass per second (14.1 kg/sec).

Figure 8. - Concluded.

At the maximum efficiency points (figs. 8(c) and (d)), the inlet temperature for the $45^{\circ}$ blockage ring increased from the hub to the tip. The maximum temperature reached near the tip was approximately $601^{\circ}$ R (333.9 K) for 0.7 $N_D$ at the maximum efficiency point. Thus, eddy flow in the tip region is indicated. However, the temperature from the hub to the blade damper was near the plenum temperature for both speeds, which indicates little mixing between the eddy flow and the mainstream flow at the maximum efficiency point. The outlet and inlet temperature profiles were similar for the $45^{\circ}$ blockage ring.

## Effect of Door Positions on Rotor Performance

The pressure-ratio and torque performance curves at 0.7 and 0.5 $N_D$ for the unblocked rotor and the rotor with simulated door positions of $20^{\circ}$, $45^{\circ}$, and $90^{\circ}$ are shown in figures 9 and 10. The performance curves for the rotor with the $90^{\circ}$ blockage ring were obtained from reference 1.

When the unblocked rotor was operated at weight flows less than the weight flows given by the surge line at speeds up to 0.7 $N_D$, unstable operation resulted, and rotating stall was present (fig. 4). However, with the $20^{\circ}$, $45^{\circ}$, and $90^{\circ}$ blockage rings, operation in the same region was stable, and there was no indication of rotating stall. Thus, several different engine acceleration modes are possible with the wide range of stable flow and pressure conditions made available with partial flow blockage.

The blade vibratory stresses (compression and tensile), as measured with strain gages attached to the rotor blades, were low for the blocked configurations. The maximum vibratory stress observed was ±5500 psi ($37.92 \times 10^6$ N/m$^2$) at 0.7 $N_D$ with the $45^{\circ}$ blockage ring. The total stress including the vibratory stress was well within the working stress range of the rotor blades. The low vibratory stress levels for the blocked configurations indicate an absence of rotating stall patterns; this was substantiated by hot-wire anemometer surveys at the rotor inlet.

The pressure ratio, torque, and weight flow may be compared for various degrees of blockage. The operating points to be used in the comparison were determined by the method presented in reference 1. The maximum efficiency operating point of the unblocked rotor is used as a reference point. The ratio of the best efficiency-point flow to the maximum flow is taken for the unblocked rotor. This ratio is multiplied by the maximum flow of the blocked rotor configurations to obtain flow operating points. These operating points are shown in figures 9 and 10 as solid symbols and might approximate an operating line for the rotor in an engine while the blockage doors are actuated from $0^{\circ}$ to $90^{\circ}$.

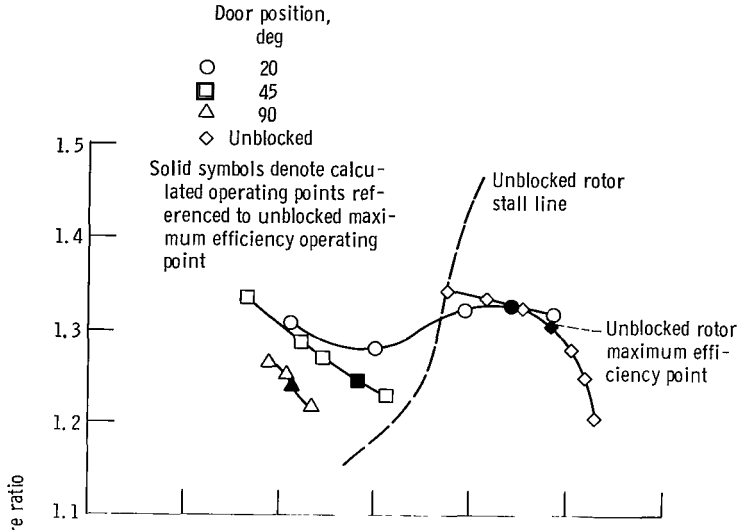


(a) Total pressure ratio as function of weight flow at equivalent speed of 0.7 $N_D$.

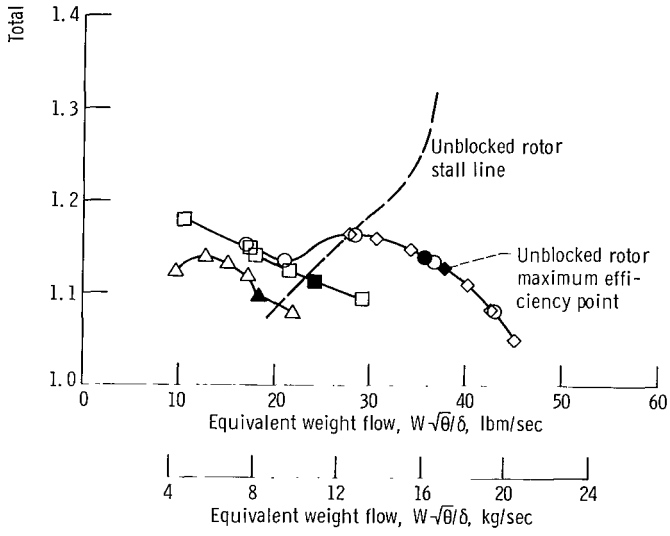


(b) Total pressure ratio as function of weight flow at equivalent speed of 0.5 $N_D$.

Figure 9. - Comparison of rotor pressure ratio for various flow blockage configurations.

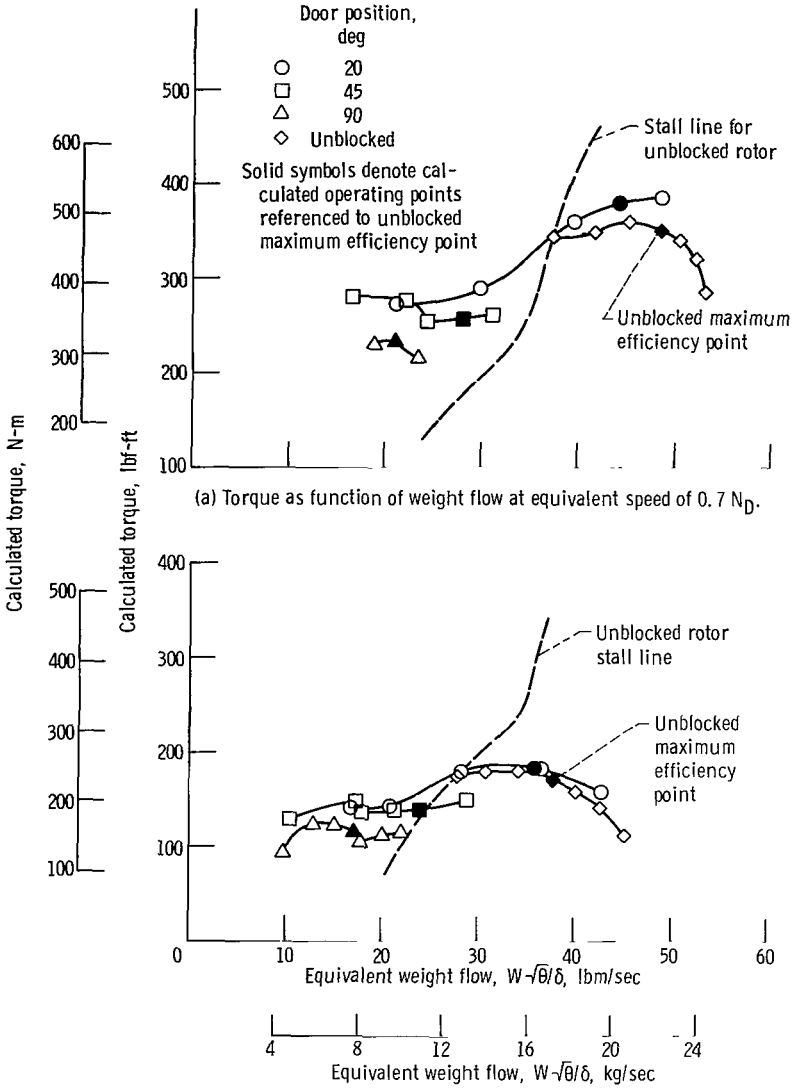


(a) Torque as function of weight flow at equivalent speed of 0.7 $N_D$.

(b) Torque as function of weight flow at equivalent speed of 0.5 $N_D$.

Figure 10. - Comparison of rotor torque for various flow blockage configurations.

Figure 9 shows the pressure ratio as a function of equivalent weight flow for the $0^o$ (unblocked) $20^o$, $45^o$, and $90^o$ blockage rings. At 0.7 $N_D$ (fig. 9(a)), the pressure ratios at the assumed operating points are 1.306, 1.327, 1.247, and 1.240 for the $0^o$, $20^o$, $45^o$, and $90^o$ blockage rings, respectively. Corresponding values at 0.5 $N_D$ (fig. 9(b)) are 1.129, 1.142, 1.113, and 1.097. Thus, the core gas generator would be subjected to a varying pressure ratio from the fan rotor as the blockage doors are actuated from $0^o$ to $90^o$.

The effect of blockage on rotor torque is shown in figure 10. At 0.7 $N_D$ (fig. 10(a)), the torque values at the operating points are 109, 74, and 66 percent of the unblocked

rotor torque for the 20°, 45°, and 90° blockage rings, respectively. Corresponding values at 0.5 $N_D$ (fig. 10(b)) are 107, 81, and 68 percent. The torque reductions for the 45° and 90° blockage rings suggest the possibility of starting the engine with the fan bypass air blocked to reduce the starting torque requirements. Such torque reductions might permit the use of smaller and, therefore, lower cost components in the starting system.

Flow reductions were also obtained for the blocked rotor at the operating points shown in figures 9 and 10. At 0.7 $N_D$, flow reductions of 9, 42, and 56 percent of the unblocked rotor flow were obtained for the 20°, 45°, and 90° blockage rings, respectively. At 0.5 $N_D$, the corresponding flow reductions were 5, 36, and 52 percent of the unblocked rotor flow. Such flow reductions, particularly for the 45° and 90° blockage rings, should result in substantial reductions in engine thrust. It appears that blocking the fan bypass air could be used as a method of controlling thrust while maintaining high engine speed. High rates of thrust recovery might then be obtained by simply opening the blocked area.

A comparison of the unblocked rotor maximum efficiency and the blocked rotor maximum efficiency is presented in figure 11. The solid curves represent the data from

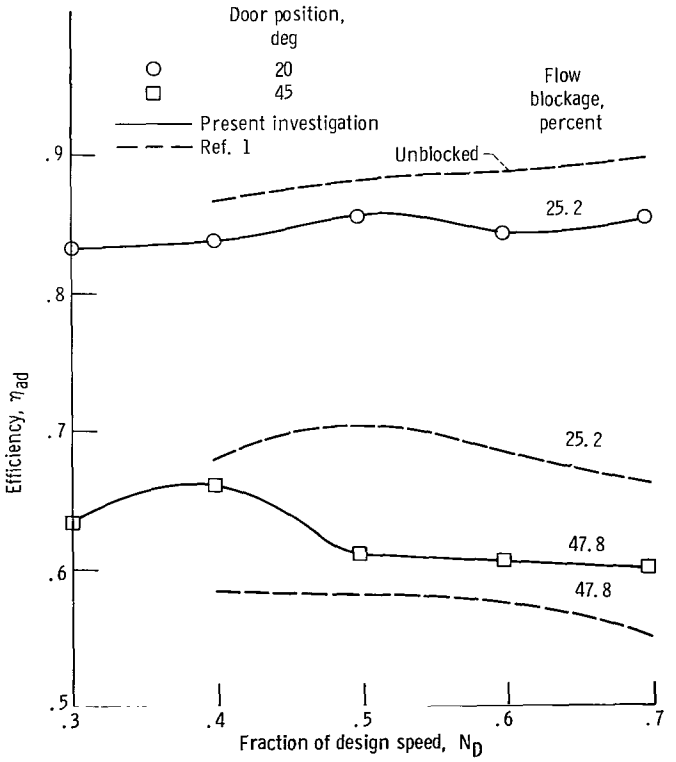


Figure 11. - Comparison of maximum efficiency for unblocked and blocked rotor configurations.

this investigation, and the dashed curves represent data taken from reference 1. With the $20^{\circ}$ ring installed, there is a small loss (2.5 to 4.5 percentage points from 0.4 to 0.7 $N_D$) in maximum efficiency as compared with the unblocked rotor maximum efficiency. For the $45^{\circ}$ blockage ring, the maximum efficiency drops 20.5 to 29.6 percentage points for the same speed range.

The effect on maximum efficiency of inserting the blockage gradually, as was done in this investigation, or abruptly (perpendicularly), as was done in reference 1 is also shown in figure 11. For 25.2-percent blockage, the loss in efficiency (as compared with the unblocked rotor efficiency) is much less for the $20^{\circ}$ blockage ring (solid curve) than for the blockage inserted perpendicularly close behind the rotor (dashed curve). For the 47.8-percent blockage, the efficiency loss for the $45^{\circ}$ ring is also less than that for the same blockage inserted abruptly, but the difference is not as marked.

The effect on rotor torque of inserting the blockage gradually or abruptly is shown in figure 12. The torque values are referenced to the unblocked maximum efficiency point as was done in reference 1. With 25.2-percent flow blockage inserted gradually as done with the $20^{\circ}$ blockage ring, the rotor torque was 109 to 106 percent of the unblocked rotor torque from 0.7 to 0.4 $N_D$. For the same blockage (25.2 percent inserted abruptly (perpendicularly) close behind the rotor (dashed curve), the rotor torque was

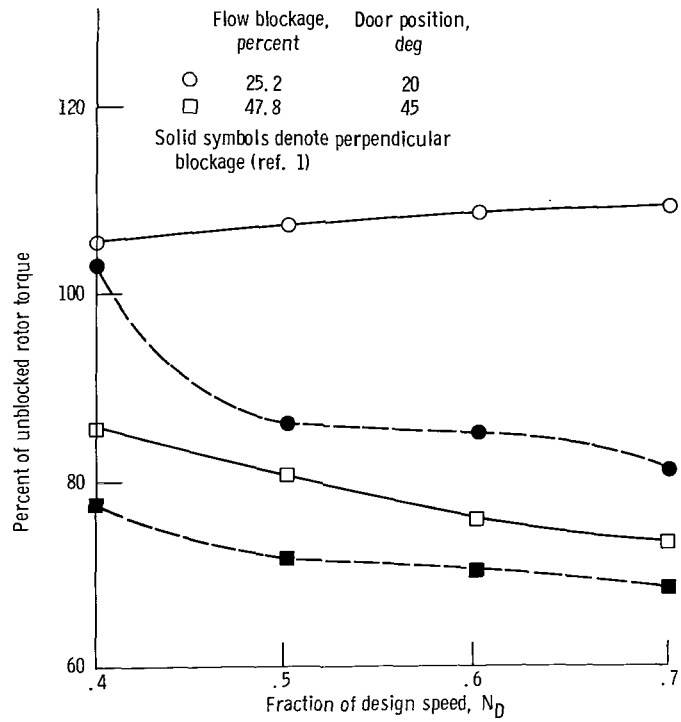


Figure 12. - Comparison of rotor torque for several flow blockage configurations. Data referenced to unblocked maximum efficiency point.

81 to 86 percent of the unblocked rotor torque from 0.7 to 0.5 $N_D$. However, at 0.4 $N_D$, the torque increased to 103 percent. For the 45° blockage ring (47.8 percent flow blockage), the torque values were 74 to 86 percent of the unblocked rotor torque from 0.7 to 0.4 $N_D$. For the same blockage (47.8 percent) inserted abruptly, the torque values were 69 to 78 percent of the unblocked rotor torque for the same speed range.

## CONCLUDING REMARKS

The blockage configurations tested in this investigation and in the investigation of reference 1 suppressed rotating stall at rotor speeds as high as 0.7 $N_D$. Suppression of rotating stall resulted in a low blade vibratory stress and enabled the rotor to operate in a stable condition to very low flows. It should be pointed out that the design tip speed for the rotor investigated is approximately 1396 feet per second (426 m/sec). Thus, the blockage data shown for 0.7 $N_D$ are for 977 feet per second (298 m/sec), at which tip speed the unblocked rotor peak efficiency was 0.896 with a pressure ratio of 1.306.

Actuating blockage doors into the air stream causes high streamline curvature of the outermost through-flow streamlines as they pass through the rotor and around the blockage. This results in low velocities near the rotor tip, which enables an eddy flow to form in this region. The eddy may have the appearance of ring stall encompassing the rotor tip. It is sufficiently axially symmetric that unsteady conditions are not imposed on the blade forces as is usually noted where rotating stall exists. Apparently this ring stall is stable enough to grow in size as the rotor back pressure and blockage are increased, and rotating stall does not occur. The losses incurred in the eddy are reflected in losses in overall efficiency and in an increase in temperature near the blade tip region. It may be necessary to limit the operating time at high degrees of flow blockage, especially at high rotational speeds, because of the high temperature in the rotor tip region. It might be possible to alleviate the high temperature condition and still maintain stable operation by allowing a small air leakage through the blocked region.

A comparison of the pressure ratios for the 0°, 20°, 45°, and 90° blockage configurations indicates small changes in the pressure ratio for this test rotor. Thus, the core gas generator would be subjected to variations in pressure ratio from the fan rotor as the blockage doors are actuated.

Since it appears that stability of operation is obtainable for the fan rotor with blockage, a device for blocking the fan bypass air could be used for obtaining several beneficial modes of engine operation. First, engine acceleration modes may be varied as a result of the wide range of stable flow and pressure conditions made available with partial flow blockage. Second, blocking the fan bypass air to reduce the rotor torque may be useful for engine startup. Such torque reductions may also allow the application of

lower cost starting equipment. Third, air flow blockage may allow operation at reduced thrust but with high engine rotational speed. High rates of thrust recovery could then be obtained by simply opening the blockage doors.

## SUMMARY OF RESULTS

An investigation was made to determine the effects of downstream flow blockage on the performance of an axial-flow fan rotor. Two fixed blockage rings were tested which simulated movable door positions of $20^{\circ}$ and $45^{\circ}$ in the bypass air duct of a turbofan engine. The following results were obtained:

1. Rotor operation was stable with both blockage rings at equivalent speeds as high as 0.7 $N_D$ (977-ft/sec or 298-m/sec tip speed). No evidence of rotating stall was detected, and the maximum blade vibratory stress observed was ±5500 psi ($37.92 \times 10^6$ $N/m^2$).

2. At 0.7 $N_D$, the lowering of simulated blockage doors from $0^{\circ}$ (unblocked) to $45^{\circ}$ changed the rotor pressure ratio from 1.306 ($0^{\circ}$) to 1.327 ($20^{\circ}$) and 1.247 ($45^{\circ}$). Corresponding values at 0.5 of design speed were 1.129, 1.142, and 1.113.

3. Losses in maximum efficiency of 2.5 to 4.5 percentage points resulted for the $20^{\circ}$ blockage ring at speeds from 0.4 to 0.7 $N_D$. For the $45^{\circ}$ blockage ring, the losses increased to 20.5 to 29.6 percentage points.

4. For the speed range 0.7 to 0.4 $N_D$, the rotor torque was 109 to 106 percent of the unblocked rotor torque for the $20^{\circ}$ blockage ring and 74 to 86 percent of the unblocked rotor torque for the $45^{\circ}$ blockage ring.

5. At 0.7 design speed, flow reductions of 9 and 42 percent of the unblocked rotor flow were realized for the $20^{\circ}$ and $45^{\circ}$ blockage rings, respectively. The corresponding flow reduction values at 0.5 design speed were 5 and 36 percent.

6. With blockage and at low flows, the inlet temperature was considerably higher at the blade tip than at the blade hub, which indicated an eddy flow or backflow near the blade tip. The eddy flow was larger for the $45^{\circ}$ blockage ring and mixed more with the mainstream flow than for the $20^{\circ}$ blockage ring. A maximum inlet temperature of $703^{\circ}$ R (390.5 K) was reached near the blade tip for the $45^{\circ}$ blockage ring at 0.7 design speed.

Lewis Research Center,
National Aeronautics and Space Administration,
Cleveland, Ohio, June 26, 1970,
720-13.

## REFERENCES


1. Osborn, Walter M.; and Lewis, George W., Jr.: Effects of Three Outlet-Annulus Area Blockage Configurations on the Performance of a 20-Inch (50.8-cm) Axial-Flow Compressor Rotor. NASA TN D-5506, 1969.
2. Huntley, S. C.; Huppert, Merle C.; and Calvert, Howard F.: Effect of Inlet-Air Baffles on Rotating-Stall and Stress Characteristics of an Axial-Flow Compressor in a Turbojet Engine. NACA RM E54G09, 1955.
3. Filippi, Richard E.; and Lucas, James G.: Effect of Compressor-Inlet Area Blockage on Performance of An Experimental Compressor and a Hypothetical Engine. NACA RM E54L01, 1955.


NASA-Langley, 1970 —— 28 E-5215

*"The aeronautical and space activities of the United States shall be conducted so as to contribute . . . to the expansion of human knowledge of phenomena in the atmosphere and space. The Administration shall provide for the widest practicable and appropriate dissemination of information concerning its activities and the results thereof."*

—NATIONAL AERONAUTICS AND SPACE ACT OF 1958

# NASA SCIENTIFIC AND TECHNICAL PUBLICATIONS

TECHNICAL REPORTS: Scientific and technical information considered important, complete, and a lasting contribution to existing knowledge.

TECHNICAL NOTES: Information less broad in scope but nevertheless of importance as a contribution to existing knowledge.

TECHNICAL MEMORANDUMS: Information receiving limited distribution because of preliminary data, security classification, or other reasons.

CONTRACTOR REPORTS: Scientific and technical information generated under a NASA contract or grant and considered an important contribution to existing knowledge.

TECHNICAL TRANSLATIONS: Information published in a foreign language considered to merit NASA distribution in English.

SPECIAL PUBLICATIONS: Information derived from or of value to NASA activities. Publications include conference proceedings, monographs, data compilations, handbooks, sourcebooks, and special bibliographies.

TECHNOLOGY UTILIZATION PUBLICATIONS: Information on technology used by NASA that may be of particular interest in commercial and other non-aerospace applications. Publications include Tech Briefs, Technology Utilization Reports and Notes, and Technology Surveys.

*Details on the availability of these publications may be obtained from:*

**SCIENTIFIC AND TECHNICAL INFORMATION DIVISION**

**NATIONAL AERONAUTICS AND SPACE ADMINISTRATION**

**Washington, D.C. 20546**